Environmental Engineering and Management Journal

January 2019, Vol.18, No. 1, 59-69
http://www.eemj.icpm.tuiasi.ro/; http://www.eemj.eu

"Gheorghe Asachi" Technical University of Iasi, Romania

EFFECT OF SYNTHESIS PARAMETERS ON SORPTIVE PROPERTIES OF GLYCEROL-DERIVED MESOPOROUS CARBON

Maria Ignat[1,2*], Liviu Sacarescu[1], Maria Emiliana Fortuna[1], Pegie Cool[3], Valeria Harabagiu[1]

[1]"Petru Poni" Institute of Macromolecular Chemistry, 41A Gr. Ghica Voda Alley, 700487 Iasi, Romania
[2]Laboratory of Materials Chemistry, Chemistry Faculty, "Al. I. Cuza" University of Iasi, Carol I Blvd., No. 11, 700506 Iasi, Romania
[3]Laboratory of Adsorption and Catalysis, University of Antwerpen (CDE), Universiteitsplein 1, 2610 Wilrjik, Antwerpen, Belgium

Abstract

The effect of synthesis conditions on sorptive properties of glycerol-derived mesoporous carbon materials were studied. Sorption properties of the synthesized carbon-based materials regarding to different adsorbate molecules, as well as water vapors, phenol and methylene blue molecules were analyzed. The sorption capacity of the synthesized mesoporous carbons depends upon synthesis conditions, namely upon pyrolyzing temperature and carbon precursor to silica weight ratio, being determined by the nature of the adsorbate molecule and the chemical and structural properties of carbon-based mesoporous material. The templated mesoporous carbons were synthesized using two different glycerol/silica weight ratios (0.5 and 1) and were pyrolyzed at various temperatures (800°C and 1000°C) to study changes in their textural, structural, morphological and chemical surface properties, as well their sorptive properties. The obtained data showed that both considered parameters, glycerol/silica weight ratio and pyrolysis temperature, are important factors in developing the carbon properties. The variation of above mentioned parameters conduct to a progressive deterioration of the carbon structure, associated with structure shrinking and pore walls breaking. Especially significant changes in the structural properties of the studied mesoporous carbon materials occurred for those heated at 1000 °C, which manifested themselves in a loss of the total pore volume. It was found that the mesoporous carbons exhibited better thermal stability reflected by the presence of residual mesopores and/or nanostructure ordering. The studies show that the adsorption of methylene blue and phenol onto glycerol-derived mesoporous carbon materials is influenced by their surface chemistry given by the synthesis conditions.

Keywords: mesoporous carbon, synthesis parameters, sorptive properties

Received: December, 2014; Revised final: May, 2015; Accepted: May, 2015; Published in final edited form: January, 2019

1. Introduction

Recently, many researches have been focused on mesoporous carbon materials due to their characteristic features as high surface homogeneity, good electrical conductivity and chemical inertness (Gierszal et al., 2008). In addition, their pore size is controllable, these materials have high surface area, and their surface properties are tailorable (Ryoo et al., 2001). Besides the electro-catalytic application (Gadiou et al., 2005; Kim et al., 2006; Wang et al., 2004), some applications in the field of hydrogen storage, super-capacitor, or adsorption of bulky molecules on mesoporous carbon materials have been found (Secula et al., 2018; Wu et al., 2008).

Mesoporous materials are promising adsorbents, because of their excellent physical and chemical properties (Kresge et al., 1992), which make them applicable in sorption processes of various molecules. Mesoporous carbon materials are of great

*Author to whom all correspondence should be addressed: e-mail: ignat.maria@icmpp.ro, maria.ignat@uaic.ro; Phone: +40746505227

research interest among the mesoporous materials due to their above mentioned exceptional properties (Palanichamy et al., 2014). The main goal of these study is to investigate the effect of synthesis parameters on sorptive properties of glycerol-derived mesoporous carbon materials prepared via template method.

Generally, mesoporous carbon materials are synthesized by hard template method and, for the first time, Ryo et al. (1999) synthesized ordered mesoporous carbon (CMK-1) using sucrose as carbon precursor and MCM-48 silica template (Carlsson et al., 1999). Subsequently, a series of ordered mesoporous carbon materials with uniform pore sizes were prepared through carbonization of polymers (furfuryl alcohol) inside the pore channels of SBA-15, MCM-48 silicas (Fuertes, 2004; Kim et al., 2003). Recently, Ignat and co-workers reported the hard template synthesis of ordered mesoporous carbon using glycerol as new carbon precursor (Ignat et al., 2010). Therefore, this work continue the research and report the study on the effect of the synthesis parameters that affect the structural, textural, morphological and sorptive properties of glycerol-derived mesoporous carbon materials. In this paper, as template was used SBA-15 silica and two parameters were considered in the hard template method, namely glycerol/silica weight ratio (of 0.5, and 1 respectively) and pyrolyzing temperature (of 800°C, and 1000°C respectively). It was found that decomposition of the carbon precursor, glycerol in this case, resulted more or less in amorphous carbon. The straight carbon nanorods were formed inside the pores of SBA-15 silica, and the carbon structure was determined by the reaction temperature and glycerol/silica weight ratio. The resulting materials were characterized using small angle X-ray scattering technique (SAXS), nitrogen adsorption-desorption measurements, scanning electron microscopy (SEM), transmission electron microscopy (TEM), thermogravimetric analysis (TGA/DTG), Fourier transform infrared spectroscopy (FTIR). The adsorption tests of water vapors, phenol, and methylene blue were performed and the obtained results are comparable with that found in the literature.

2. Experimental

2.1. Synthesis of mesoporous carbon materials

In this paper, the mesoporous carbons are prepared via hard template method using SBA-15 silica as template. The synthesis of SBA-15 silica template was performed according to a method proposed by Hartmann and Vinu (2002). Two different parameters as glycerol/silica weight ratio (of 0.5 and 1 respectively) and pyrolysing temperature (of 800°C, and 1000°C respectively) were considered for the synthesis of mesoporous carbon materials.

In a typical experiment for the synthesis of mesoporous carbon materials, 1 g of mesoporous silica powder, SBA-15, was impregnated with a glycerol solution of different concentrations in order to achieve the glycerol/silica weight ratios of 0.5 and 1, respectively. The obtained mixtures were then subjected to the polymerization in the oven for 6 h at 100°C, then the temperature was raised up to 160°C for other 6 h (1°C/min) in order to obtain a full polymerized glycerol inside silica channels. The silica-polyglycerol powder was then subjected to pyrolysis in a N_2 flow, at 800°C (8) or 1000°C (10), respectively, for 5 h, in order to carbonize the polymer inside silica pores. After that, the silica template have been removed with 10% HF solution, and the black solid was then filtered, washed with distilled water three times, with ethanol and dried at room temperature. The obtained samples were labeled as xC8 and xC10 (x = glycerol/silica weight ratio).

2.2. Characterization techniques

Small angle X-ray scattering was used to characterize the nanometric structure of the powdered sample phase. The data were collected on a Bruker-Nanostar U apparatus equipped with a 3-pinhole collimation system providing a precisely parallel X-ray beam with high intensity and virtually no background, achieving fast measuring times and extremely high resolution. The scattering intensity was measured as a function of scattering vector, q, being defined as $q = (4\pi/\lambda)\sin\theta$, where 2θ is the scattering angle and λ is the X-ray wavelength (1.54 Å). The SEM images were obtained using a JSM 5510 microscope, operating at an accelerating voltage of 15 kV. The TEM measurements were performed using a HITACHI T7700 microscope operated at 120 kV, using copper grids (300 mesh) coated with ultrathin carbon film on holey carbon support film (Ted Pella, Redding, CA). The textural properties of the carbon samples were determined by a Quadrasorb SI (Quantachrome) automated gas adsorption system using nitrogen as adsorbate at -196˚C. All samples were out gassed for 16 h at 200 ˚C. The specific surface area was estimated from the BET equation. The total pore volume was taken at $P/P_0 = 0.95$. Pore size distributions (PSDs) were determined using Barrett-Joyner-Halenda equation (Barrett et al., 1951). Thermogravimetric experiments were performed on a Mettler TG-50 thermobalance connected to a TG 10A processor at a heating rate of 5°C/min, and under oxygen flow. The surface chemistry of the obtained materials was investigated by Fourier-Transform Infra-Red spectroscopy (FT-IR) performed on a Nicolet Nexus spectrometer equipped with a MCT/B detector. The samples were mixed with KBr and compressed into pellets.

2.3. Sorption experiments

Water adsorption isotherms were collected with a home-built volumetric sorption system gifted with a rotary vane pump and a turbomolecular pump, which pressure transducer range is 1–1000mbar (resolution 0.1 mbar). Water adsorption data were obtained at room temperature for all samples using the

same sample holder. A small amount of pure water was introduced in a tank, which was then evacuated for air removal, leaving a saturated water vapor atmosphere. The sample holder was connected to the water vapor tank through a glass tube gifted with valves, which allow the control of the relative humidity of the sample environment. Water vapor isotherms were obtained by setting pressure intervals relative to the saturation vapor pressure. Prior to measurements, samples were out gassed for 16 h at 200˚C. 50 mL of methylene blue (MB) and phenol (Ph) standard solutions with predetermined initial concentration of 10, 20, 30, 40, and 50 mg/L were taken in the 100 mL conical flasks containing 0.01 g of carbon sample. In order to prevent sunlight from causing color bleaching, the flasks containing mixtures were kept in a dark box, stirring them continuously for 12 hours. Then, the solution was filtrated and the clear supernatants were then analyzed using a UV-Vis spectrophotometer (Shimadzu 2401) at their maximum wavelength. Also, the liquid/solid ratio have been varied and was found that 0.01 g of solid is the optimum mass for adsorption process.

3. Results and discussion

3.1. Structural characteristics of carbon materials

Fig. 1 shows the small-angle X-ray scattering patterns of templated carbon materials synthesized from different glycerol/silica weight ratios being carbonized at 800°C and 1000°C, respectively

The SAXS patterns of carbon samples show three peaks, corresponding to (100), (110) and (200) reflections indicating a 2D hexagonal space group p6mm (Zhang et al., 2002). The (100) peak is positioned at around 1° and allows to calculate the interplanar distances and unit cell parameters, while the (110) and (200) long order weak peaks are positioned in the range of 1.5°-2.0°, confirming that the synthesized mesoporous carbon materials retained the hexagonal structure of the silica template. All SAXS intensity profiles are the product of the cylinder form-factor for the individual pores. Because there is no possibility to dilute such systems, the general intensity profiles for an assembly of parallel pores is very complex. The general shape of SAXS profiles characterizing synthesized mesoporous carbon materials is similar for all samples. A regular pattern is clearly defined covering the s-range from 0.05 to 0.2 nm^{-1}, but a little bit displaced to different s values for each sample. For example, the mesoporous carbon prepared from the 0.5 glycerol/silica ratio, 0.5C800 sample, provided the first broad peak at a value of s of approximately 0.08 $Å^{-1}$ (d = 7.8 nm) with second-order reflections at $3^{1/2}$s that correspond to the short-range order of a hexagonally packed cylinder structure (this result is consistent with the TEM image shown in Fig. 5, which displays a rod-like structure).

The same procedure has been applied for all carbon samples and the calculated unit cell parameters and corresponding interplanar distances are summarized in Table 1. These features arise from Bragg peaks (Fig. 1) in the structure factor from the two-dimensional hexagonal array of pores. The Bragg peaks are broad and could not give the full range of sharp peaks characterizing a perfect hexagonal lattice, meaning that there are areas with disordered pores.

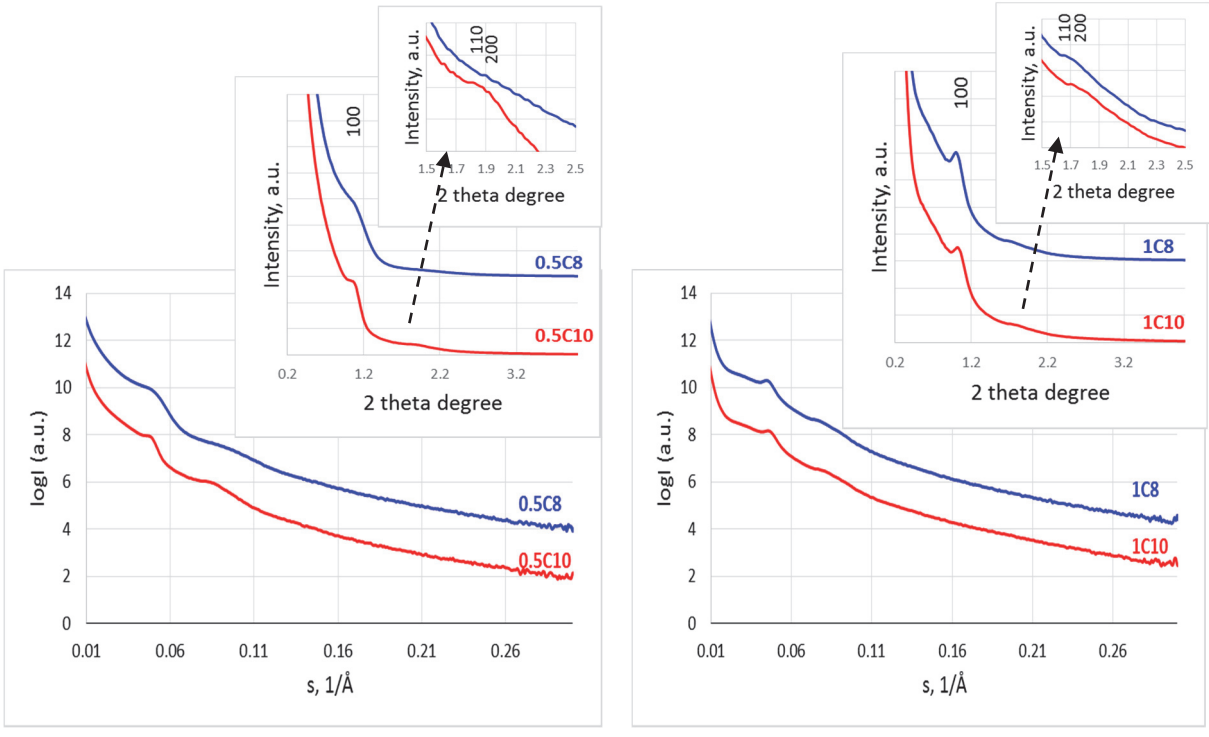

(a) (b)

Fig. 1. SAXS profiles of 0.5C8, 0.5C10 (a), 1C8, and 1C10 (b) carbon samples

Table 1. Textural and structural characteristics of the synthesized mesoporous carbon materials in different conditions

Sample / *Parameter**	*0.5C800*	*0.5C1000*	*1C800*	*1C1000*
S_{BET}, m^2/g	1138	1150	1370	1390
V_{tot}, cc/g	1.34	1.1	1.5	1.03
V_{micro}, cc/g	0.022	0.038	0.025	0.035
S_{micro}, m^2/g	54	82	78	97
Mesoporosity, %	95	92	94	92
d_p, nm	3.5	2.7; 3.75	4.0	2.7; 3.7
***d_{100}*, nm**	7.8	8.2	8.7	8.4
***a_0*, nm**	9.1	9.5	10.0	9.8
***W_t*, nm**	5.6	6.8; 5.75	6.0	7.1; 6.1

Note: S_{BET} is apparent surface area calculated by the BET method; V_{tot} - total pore volume calculated as the amount of nitrogen adsorbed at a relative pressure of $P/P_0 = 0.95$; V_{micro} - micropore volume calculated by the t-plot method; S_{micro} - micropore surface area calculated using t-plot method; Mesoporosity is the percentage of mesoporous surface area from the apparent surface area; d_p- average pore diameter resulted from BJH method using adsorption branches; d_{100} - the d-spacing values were calculated by the formula $d_{100}=\lambda/2\sin\theta$ from the SAXS profile; a_0 - unit cell parameter determined from SAXS using the formula $a = 2 * 3^{-1/2} d_{100}$; W_t - pore wall thickness calculated by substracting the BJH pore size from the unit cell parameter.*

At the first look, is easy to observe that with increasing pyrolyzing temperature this reflections shift a little bit to higher 2θ values, indicating a variation of the interplanar distance and unit cell parameter, respectively. $I_{(100)}/I_{(110)}$ ratio also changes with increased pyrolysis temperature, indicating that the regular arrangement of pores is modified.

3.2. N_2-sorption properties of carbon materials

The nitrogen adsorption-desorption isotherms for all synthesized mesoporous carbon samples, shown in Fig. 2, are of type IV characterizing mesoporous materials with cylindrical pores**.**

Analyzing all isotherms, it was found that the adsorption capacity decreased and the position of the capillary condensation step is shifted to lower relative pressures as the pyrolyzing temperature increases. By altering the conditions for the synthesis of carbon materials, it was found that the pyrolyzing temperature plays an important role for controlling the pore size during the carbonization step. Adsorption analysis (the BET specific surface area, and the pore diameter) (Table 1) indicates that the smallest pores and the highest surface area were obtained for highest pyrolyzing temperature and highest glycerol/silica weight ratio. This can be attributed to the fact that the temperature increase may result in the increase of quantity of volatile compounds released from inside of the carbon structure as result of the decomposition process of carbon precursor (Bouchelta et al., 2012). This phenomenon has been also observed by Soltani et al. (2013) demonstrating that a modified porous carbon with a high surface area is obtained when the carbonization temperature is increased.

Comparing the pore size distribution of the synthesized samples, it could be observed that there are also some differences. Carbon materials synthesized at 800°C exhibit a uniform pore size distribution, while the pore size distributions of samples carbonized at 1000°C are non-uniform. This is explained in terms of both glycerol filling effect and silica template shrinkage during thermal treatment. Thus, as one may see from the corresponding pore size distributions (Fig. 2), the peak characterizing the average pore diameter become narrow with the increase of the carbonization temperature. This means that at high temperatures are obtained mesoporous carbon frameworks with more uniform pores. In both cases of glycerol/silica weight ratios, a second peak is observed, centered at about 2.7 nm, indicating a clear bimodal porosity of the carbon materials synthesized at higher temperature. The bimodal porosity could be assigned to the carbon samples prepared at lower temperatures, but is not the case of the synthesized samples in this work. In this case the corresponding pore size distributions exhibit wide peaks, suggesting the presence of pores of different diameters varying from 1.5 nm to 5 nm for 0.5C8 sample, and from 2 nm to 7 nm for 1C8, respectively. This is understandable since the high temperature can result in much more shrinkage of silica structure (Vaudreuil et al., 2001).

The micro-mesoporous structure is characteristic to all synthesized carbon materials no matter the pyrolysis temperature and/or glycerol/silica ratio. Therefore, analyzing the resulted micropore volumes and calculated mesoporosity, a clear trend could be observed. Thus, an enhanced microporosity in the carbon structure with increasing pyrolyzing temperature is observed. However, the involved of 0.5 glycerol/silica weight ratio in the synthesis of mesoporous carbon material led to a greater increase of microporosity, of 1%, compare to glycerol/silica weight ratio of 1. The greater micropore volume is explained by the glycerol filling effect, i.e., the silica pore are not completely filled with carbon when glycerol/silica weight ratio is 0.5 and after carbonization, this effect is responsible for the formation of micropores through carbon structure. Considering the calculated unit cell parameters, as a result of SAXS measurements, and the mean pore diameter, taken as the maximum from the BJH pore size distributions, it was possible to calculate the pore wall thickness. It was expected that, with the increase of glycerol/silica ratio, the pore wall thickness increases also, as is shown in Table 1.

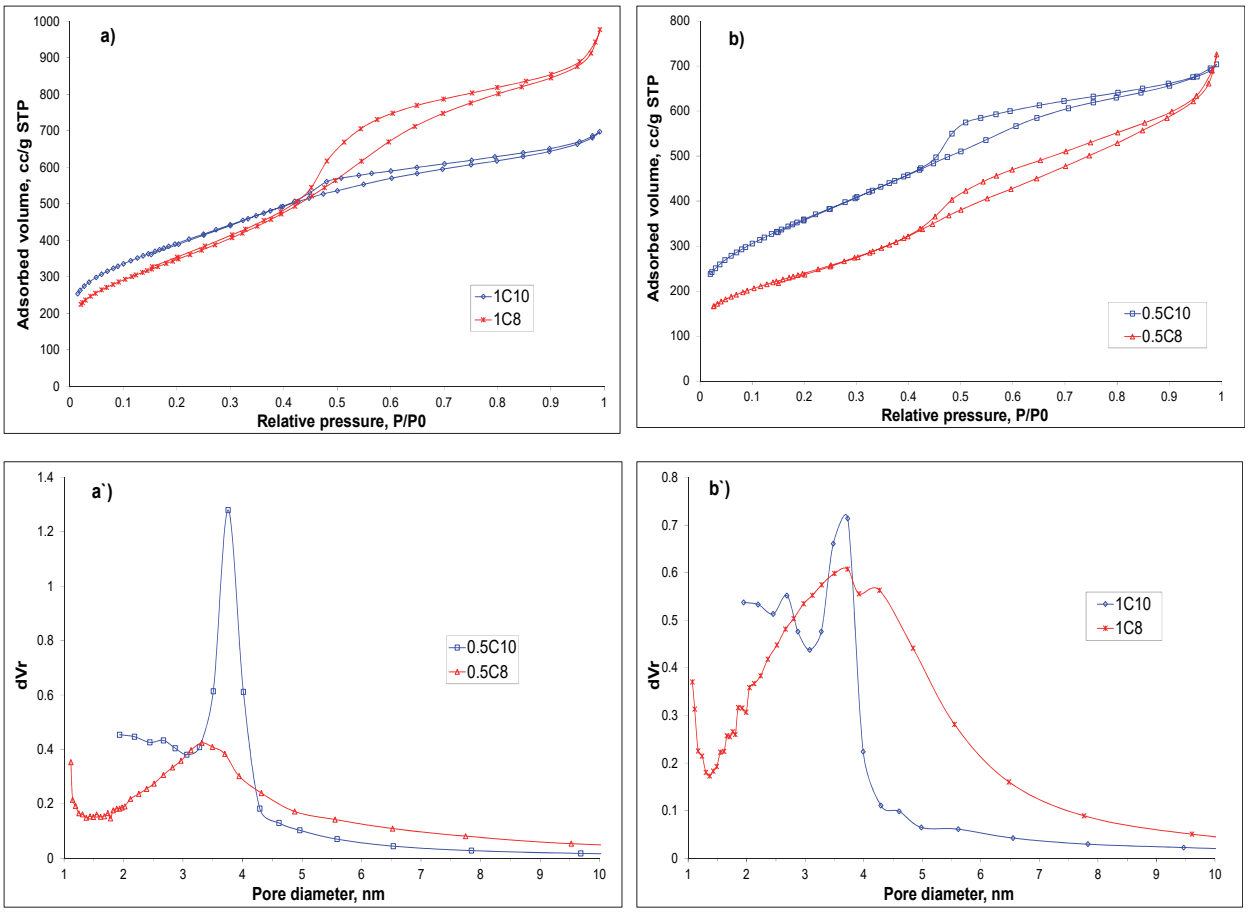

Fig. 2. Nitrogen adsorption isotherms and corresponding pore size distributions of 0.5C8 and 0.5C10 (a), 1C8 and 1C10 (b) carbon samples

As observed from the Table 1, interesting is to find out that the temperature has a beneficial effect on the wall thickness, the carbon walls becoming thicker with the increase of the pyrolyzing temperature.

3.3. Investigation of thermal stability

Thermal gravimetric analysis (TGA) is the effective way to assess the crystallinity and purity of mesoporous carbon materials by testing their thermal stability under oxidative conditions. The Fig. 3 shows the TGA/DTG curves recorded on the synthesized mesoporous carbon materials. As observed, significant difference in oxidative mass change occurs between carbon samples prepared in different manner, and the dominant weight loss step is due to the burning out the carbon as CO_2. Under air atmosphere, the TGA curves show a single step of degradation. The first part of curves corresponds to the removal of moisture with a total loss of about 4%. At the end of experiment, when temperature was raised up to 600°C, the carbon materials were completely burnt off in oxygen atmosphere. The dominant weight loss occurs in the range of 500-550°C, due to the removal of the carbon species from the system with a total degradation of about 86%. Finally, less than 10% of residue remains unburnt, in the case of 0.5C1000 carbon sample, meaning that this is the only sample that may still contain incompletely removed silica. The other synthesized carbon samples contain less than 2% of residues, indicating that a large extent of the silica template has been removed from the system.

The narrow peaks found in the range 500-630°C present in the first-derivative weight loss curves (DTG) are due to the combustion, where the carbon species were removed as CO_2 gas.

With respect to the gasification temperature of the commercial graphite (being in the range of 520 - 680°C), the gasification temperatures of the synthesized mesoporous carbons is found to be somehow similar. Thus, the graphitization process of the synthesized carbon occur almost completely at the used pyrolyzing temperatures. As could be seen in the Fig. 3, the DTG curve of the obtained 0.5C8 carbon sample, exhibit a narrow strong peak indicating that the decomposition of this sample occurs in a single stage.

Contrariwise, the DTG curve of 1C8 carbon sample exhibit two peaks, suggesting that the decomposition of such carbon occurs in two stages: one high peak at low temperature and another at higher temperature (as a shoulder), indicating different bonded carbon in the framework. As observed, the DTG peaks of the carbon samples synthesized at higher temperatures widens and are centered at 580°C, increasing their thermal stability.

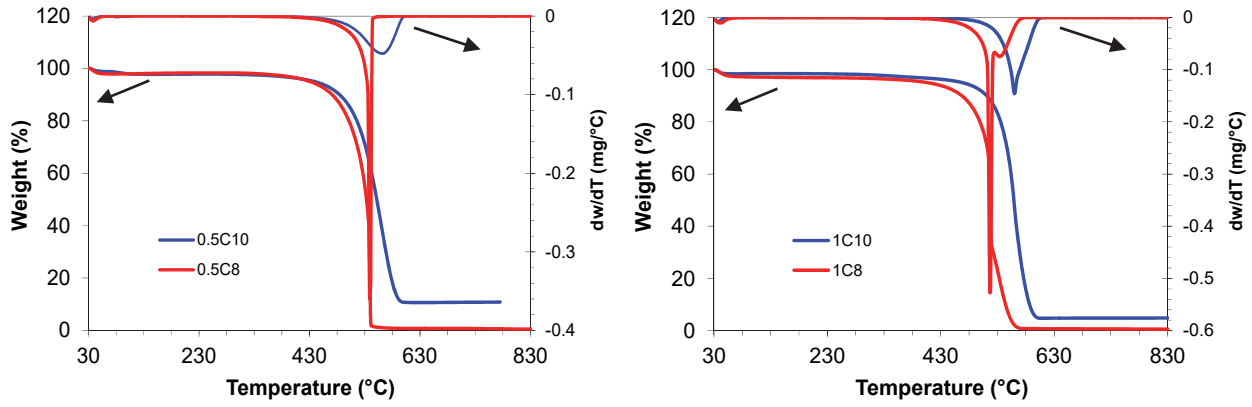

(a) (b)

Fig. 3. TGA and corresponding DTG curves for the synthesized mesoporous carbons obtained from (a) 0.5 and (b) 1 gram of glycerol

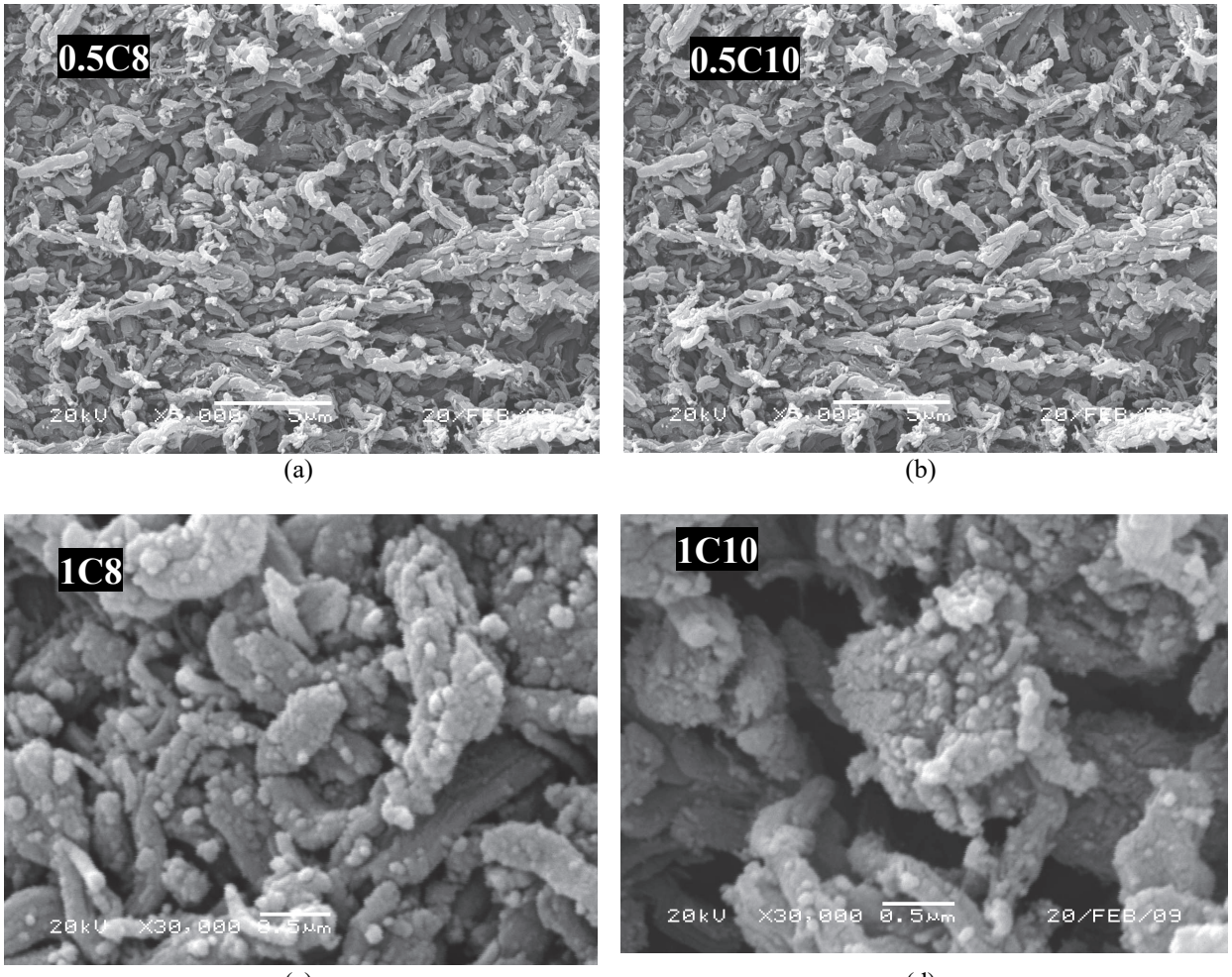

(a) (b)

(c) (d)

Fig. 4. SEM images of the synthesized mesoporous carbon materials ((a) 0.5C8, (b) 0.5C10, (c) 1C8, (d) 1C10)

The DTG peaks centered at 50°C are assigned to the desorption of physically adsorbed carbon species and/or the polymerization of glycerol because it begins to polymerize in the presence of acid catalyst at temperatures lower than 100°C (Fitzer and Schäfer, 1970; Martin and Richter, 2011). Therefore, in this case, probably the amount of partially graphitized species is diminished. One could be mentioned that the DTG curves of the samples prepared at higher temperature (1000°C) show higher peaks than that prepared at lower temperatures (800°C) resulting in the homogeneity of the carbon bonds. In conclusion, the thermal stability of the carbon materials decreases when a larger amount of glycerol is used in the carbon synthesis. Likewise, the calculated pore wall thickness increases with pyrolyzing temperature, and this could

be a plausible explanation for the decrease of the thermal stabilization of the carbon material.

3.4. Morphology of synthesized mesoporous carbons

Fig. 4 shows the SEM images of the glycerol-derived mesoporous carbon materials synthesized at different temperatures using two glycerol/silica weight ratios. SEM images confirm that the templated mesoporous carbons display more or less a morphology of bundled rod-like particles.

Additionally, the high-magnification SEM images of the synthesized carbon samples show that the carbon particles are segregated, indicating that the conglutination of the carbon particles did not occur during the pyrolysis process. But, actually, the particle conglutination has been already identified as a serious problem when a liquid carbon precursor is used in a template synthesis (Kim et al., 2005). The carbon particles conglutination at high pyrolyzing temperatures could be attributed to the silica template shrinkage during the thermal treatment.

Fig. 5 show TEM image of 1C8 carbon sample, exhibiting clearly large domains with well-ordered hexagonal arrays of pore channels, which are similar to the structure of CMK-3 type of mesoporous carbon reported elsewhere (Joo et al., 2001).

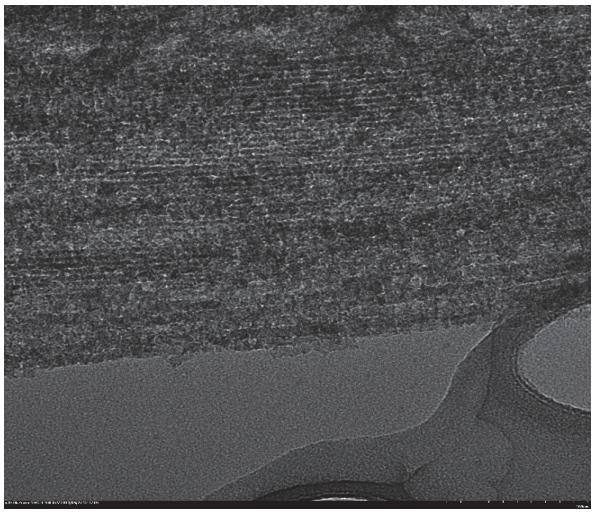

Fig. 5. TEM image of 1C8 mesoporous carbon sample

3.5. Surface chemistry analysis

Firstly, in order to prove that the polymerization of glycerol is accomplished at 160 °C, the FTIR spectra of intermediates S-gli (glycerol-impregnated silica) and S-POL (polymerized glycerol on silica surface) were recorded and the collected spectra are shown in Fig. 6.

In the FTIR spectrum of S-gli the band at 3323cm^{-1} is attributed to the hydroxyl stretching vibration. The relative intensity of this band indicates the presence of the intermolecular hydrogen bonds between molecules. As expected, other characteristic bands are those at 1425cm^{-1} and 1337cm^{-1} corresponding to bonded primary and secondary alcohols and at 673 cm^{-1} corresponding to -OH group out-of-plane deformation vibration. The bands at 2937 cm^{-1} and 2883 cm^{-1} are assigned to asymmetric and symmetric –CH_2 stretching vibrations, while the band at 1032 cm^{-1} is attributed to Si-O from silica template.

Further, knowing that by acid-catalyzed condensation of glycerol allowed to obtain a polyether product (Dube and Salehpour, 2012), the polymerized glycerol on silica surface was investigated. Thus, in the FTIR spectrum of the sample S-POL, the disappearance of the specific band assigned to primary alcohols at 1425 cm^{-1} confirms the condensation reaction. The characteristic band for the ether bond is overlapping with Si-O groups in the 1085-1120 cm^{-1} spectral range. Other bands are those at 3381 cm^{-1} and at 1630 cm^{-1} attributed to the hydroxyl groups specific for the secondary alcohols from the structure.

The surface chemistry of glycerol-derived mesoporous carbon materials were characterized by FTIR spectroscopy, and collected spectra are shown in Fig. 7. Because all samples have been dried prior analysis at 200°C, for 2 h, the FTIR spectra do not exhibit any strong band in the range 3400-3440cm^{-1}(Li et al., 2006; Xiao and Thomas, 2006), meaning that the retained water molecules on the carbon surface have been removed during the thermal treatment. The small bands at 2920 and 2854 cm^{-1} are originated from the stretching vibration of C-H alkyl bond, and also their presence is confirmed by the observed shoulder in the range of 750-900cm^{-1}(Serrano et al., 1999). The band at 1620 cm^{-1} is characteristic to C=C vibrations in terminal olefinic C=C bonds (Xiao and Thomas, 2006). The band at 1725 cm^{-1} is attributable to C=O vibrations in carboxylic group (Joo et al., 2001; Li et al., 2006). The band at 1380 cm^{-1} is ascribable to –CH_2 or –CH_3 groups (Serrano et al., 1999). There is also a broad characteristic band for C-O stretching vibrations observed in the range 900-1300 cm^{-1} coming from alcoholic, phenolic or carboxylic functional groups (Kim et al., 2005; Li et al., 2006). The broadness of this peak is due to the overlapping of various bands of functional groups. For exaample the band at 1100 cm^{-1}, may be due also to O-H bending in the structure of carboxylic groups (Joo et al., 2001).

Therefore, at the used pyrolyzing temperatures, the glycerol is polymerized and turned to aromatic structures. An increase of the polyaromatic order of glycerol-derived mesoporous carbon materials with increasing pyrolyzing temperature was observed, as demonstrated by increasing band intensity at 1620cm^{-1}. These results explain the higher thermal stability of the carbon samples synthesized at higher temperatures, as have been demonstrated by TGA/DTG measurements. As FTIR spectra confirm that there are many functional groups distributed at the surface of the glycerol-derived mesoporous carbons, and these functional groups are responsible for the improvement of the hydrophilicity and wettability of carbon materials, water adsorption measurements have been done.

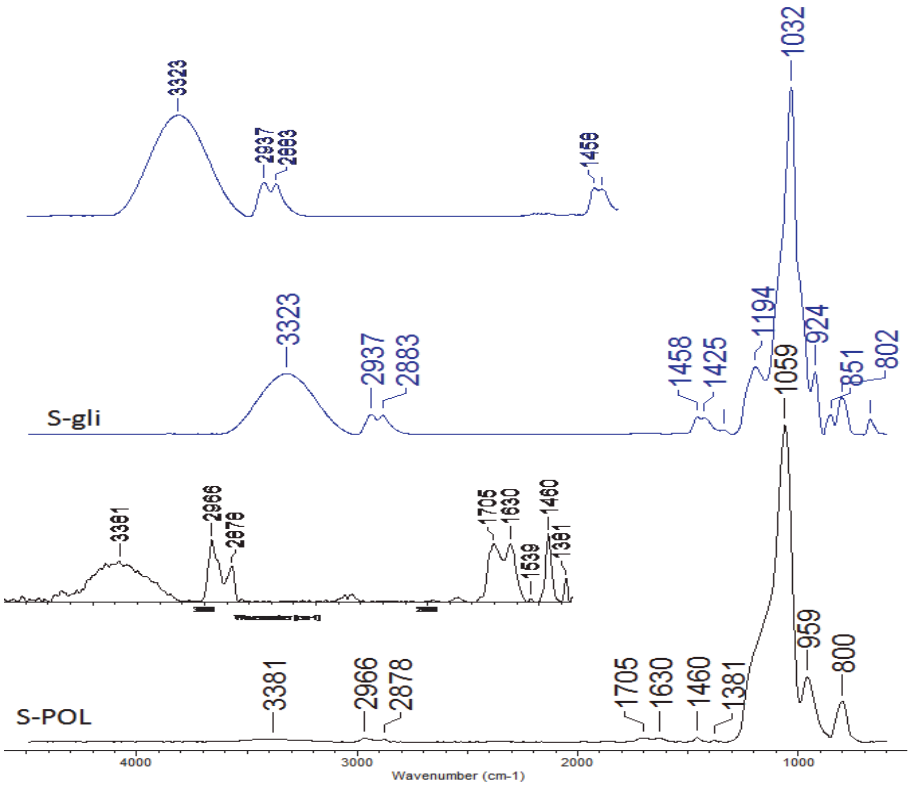

Fig. 6. FTIR spectra of S-gli (glycerol-impregnated silica) and S-POL (polymerized glycerol on silica surface)

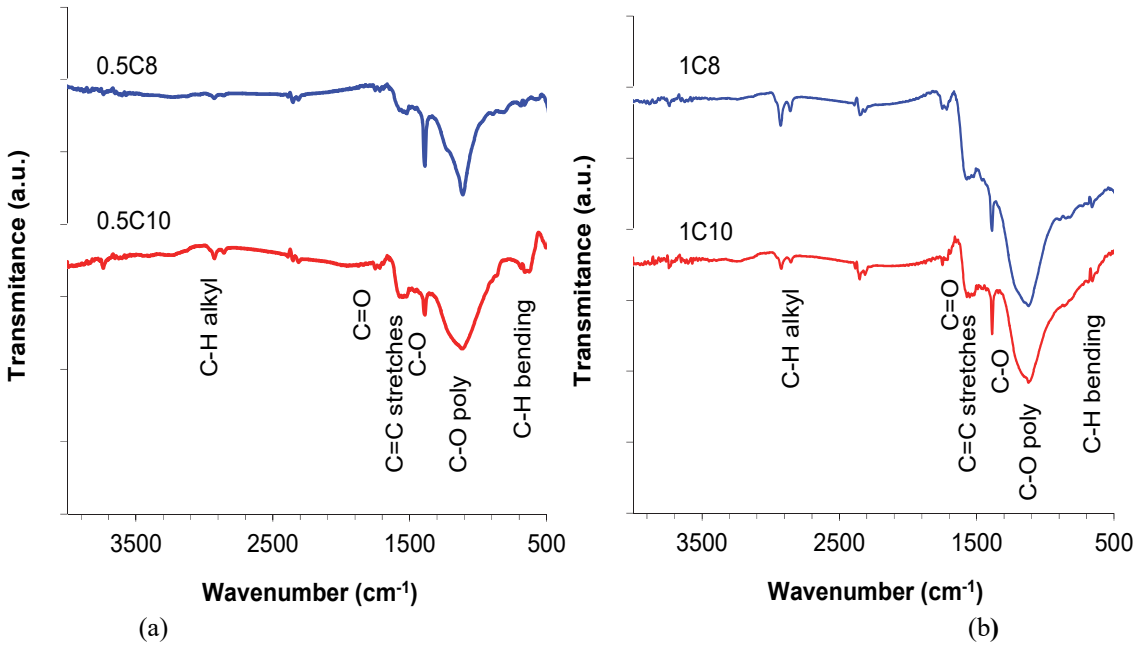

Fig. 7. FTIR spectra of dried mesoporous carbon materials synthesized in different conditions: 0.5C8/0.5C10 (a) and 1C8/1C10 (b)

This important feature of the mesoporous carbon material is advantageous for many applications as water/air purification (Suzuki, 1994), energy storage (Burchell, 1999) haemoperfusion (Guo et al., 2009), supercapacitor (Frackowiak et al., 2000; Hwang and Hyun, 2004) etc. Thus, water adsorption isotherms are shown in Fig. 8, which are of type V characteristic to porous carbon. The water adsorption isotherms of glycerol-derived mesoporous carbons show that even at low pressures a significant uptake of water vapors occurs. This behavior is a consequence of the carbon-water interactions, when active sites are present on the carbon surface. The adsorption isotherms agree qualitatively with experimental data obtained from FTIR measurements and the water sorption mechanism can be explained as the

following: at low pressures, water uptake occurs via the bonding of isolated water molecules to the oxygen-containing surface groups. It is well known that the water adsorption on a carbon surface without surface sites does not occur. Further, as the relative pressure is increased, the adsorption process occurs either directly to a surface site or to other water molecules already adsorbed at low relative pressures.

Afterwards, when all surface sites are covered by a cluster of water molecules, only a little further uptake occurs until near saturation point. However, the carbon samples synthesized at low temperatures (800°C) adsorb less water vapors than those pyrolyzed at higher temperatures (1000°C), and, as the pyrolysis temperature increases, the inflexion point is shifted towards lower relative pressures. This most likely is due to a slight increase of the specific surface area, as well as increase of the micropore volume of the 0.5C10 and 1C10 carbon samples.

3.6. Sorption results

In order to prove the sorptive properties of the synthesized carbon materials and point out that the synthesis conditions are very important, we were looking for some possible applications as sorbents for phenols and dyes from aqueous solutions (Apreutesei et al., 2009; Idris et al., 2017). Firstly, because the Infrared Spectroscopy provided a valuable information on the functionalized carbon surface, the synthesized mesoporous carbon materials were tested in the sorption process of Methylene Blue from aqueous solution. The obtained results are great compare to other porous carbon structures reported in the literature (Table 2).

Also, as on the carbon surface are non-functionalized areas, giving them the hydrophobic character, phenol sorption experiments have been run. In the Fig. 9 is shown the phenol adsorption results obtained on the most hydrophobic mesoporous carbon material synthesized in this work.

4. Conclusions

In this paper, structural, textural, and morphological properties of glycerol-derived mesoporous carbon materials in different synthetic conditions were studied. It was found that decomposition of the polymerized carbon precursor, glycerol in this case, resulted in amorphous carbon. The straight carbon nanorods were formed, and their structures were determined by two parameters: the reaction temperature (800°C and 1000°C) and glycerol/silica weight ratio (0.5 and 1).

As result, the rod-like structured carbon materials exhibit cylindrical pores ordered in a hexagonal symmetry, being limited this way by the silica pores.

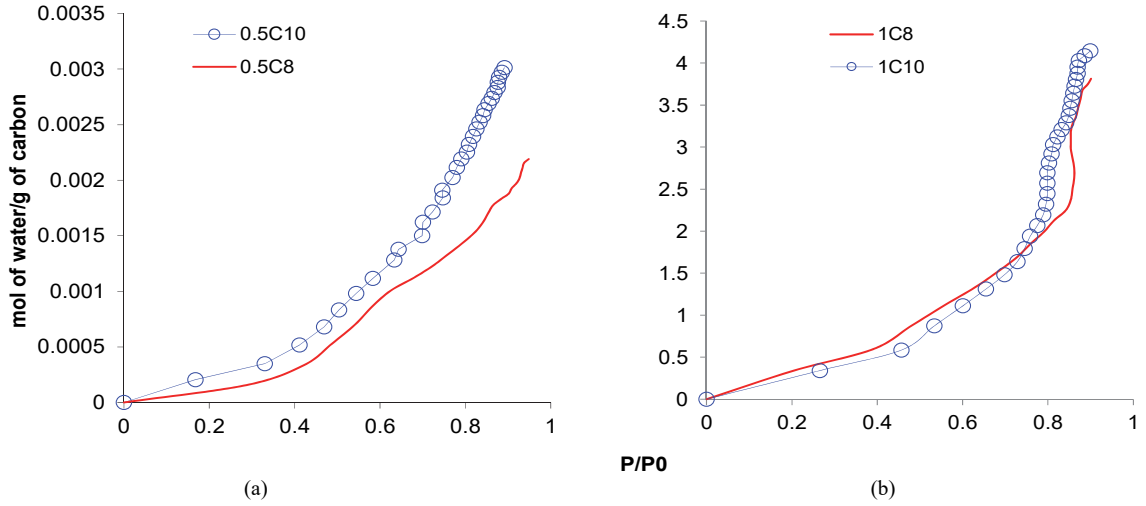

Fig. 8. Water adsorption isotherms at 25 °C on glycerol-derived mesoporous carbon samples: 0.5C8, 0.5C10 (a) and 1C8, 1C10 (b)

Table 2. Comparison of the sorption capacities of the obtained glycerol-derived mesoporous carbon materials with that of other carbons reported in the literature

Sample	*Water adsorption capacity, mmol/g*	*Phenol adsorption capacity, mg/g*	*Methylene blue adsorption capacity, mg/g*	*Reference*
0.5C8	0.0022	102	582	This work
0.5C10	0.0032	98	650	This work
1C8	3.9	58	675	This work
1C10	4.3	53	687	This work
Activated carbon	-	18	410	Shawabkeh and Abu-Nameh (2007)
Activated carbon	-	97	-	Karabacakoglu et al. (2008)
Activated carbon	-	-	590	Abdulkarim et al. (2002)
Carbon nanotubes	-	-	580	El Qada et al. (2006)

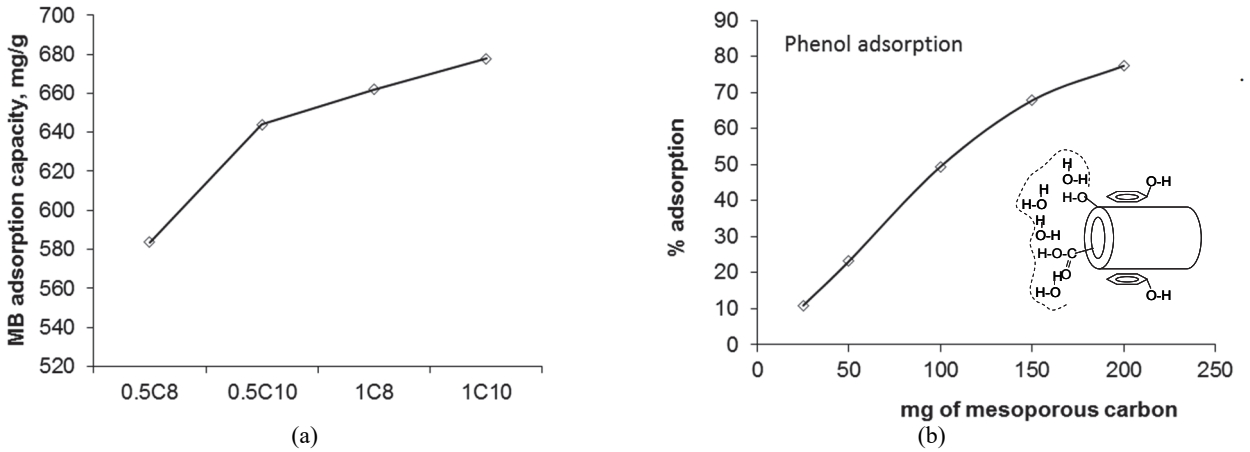

Fig. 9. Methylene blue adsorption capacities for the synthesized mesoporous carbon materials (0.5C8, 0.5C10, 1C8, 1C10 samples) and Phenol adsorption on 0.5C8 sample

The increase of the pyrolyzing temperature results in a decrease of the structural parameters modifying the regular arrangement of pores. The increase of the pyrolyzing temperature and the glycerol/silica weight ratio lead to an increase of the total specific surface area, as well as the micropore surface area.

Nitrogen sorption measurements showed that the smallest pores and the highest specific BET surface area were obtained for the highest pyrolyzing temperature and highest glycerol/silica weight ratio. Thus the temperature increase results in the increase of quantity of volatile compounds released from inside of the carbon structure as the result of decomposition of the carbon precursor, thus reducing mesoporosity of the carbon material and enhancing its microporosity. Also, it was demonstrated that the investigated parameters have an effect on the carbon surface chemistry and thermal stability. Regarding adsorption of water vapors on the surface of synthesized carbon materials, the increase of pyrolyzing temperature results in a slight increase in the amount of adsorbed water. These results of sorption experiment suggest that the water adsorption depends on both the surface chemistry and specific surface area of the synthesized glycerol-derived mesoporous carbon materials.

Once the surface have been characterized, the sorptive properties of the synthesized mesoporous carbon materials were tested. As result, comparable or even higher sorption capacities for phenol and methylene blue were obtained. In conclusion, the glycerol-derived mesoporous carbons synthesized via template-assisted method have great surface properties that make them good sorbents for organic molecules.

Acknowledgements

This work was supported by a grant of the Romanian Ministry of Education, CNCS – UEFISCDI, project number PN-II-RU-PD-2012-3-0357, Contract 30/2013, and project number PN-II-ID-PCE-2011-3-0559, Contract 265/2011 for the financial support. The authors gratefully acknowledge G. Van Tendeloo (EMAT, UA, Antwerpen, Belgium) for the SEM measurements.

References

Abdulkarim M.A., Darwish N.A., Magdy Y.M., Dwaidar A., (2002), Adsorption of phenolic compounds and methylene blue onto activated carbon prepared from date fruit pits, *Engineering in Life Sciences*, **2**, 161-165.

Apreutesei R.E., Catrinescu C., Teodosiu C., (2009), Studies regarding phenol and 4-chlorophenol sorption Y surfactant modified zeolites, *Environmental Engineering and Management Journal*, **8**, 651-656.

Barrett E.P., Joyner L.G., Halenda P.H., (1951), The determination of pore volume and area distributions in porous substances. Computations from nitrogen isotherms, *Journal of the American Chemical Society*, **73**, 373-380.

Bouchelta C., Medjram M.S., Zoubida M., Chekkat F.A., Ramdane N., Bellat J.P., (2012), Effects of pyrolysis conditions on the porous structure development of date pits activated carbon, *Journal of Analytical and Applied Pyrolysis*, **94**, 215-222.

Burchell T., (1999), *Carbon Materials for Advanced Technologies*, Pergamon Publishing House.

Carlsson A., Kaneda M., Sakamoto Y., Terasaki O., Ryo R., Joo S.H., (1999), The structure of MCM-48 determined by electron crystallography, *Journal of Electron Microscopy*, **48**, 795-798.

Dube M., Salehpour S., (2012), Methods of Making Polyglycerol. USA Patent, WO *2012123777 A1*.

El Qada E.N., Allen S.J., Walker G.M., (2006), Surface modification effects on CNTs adsorption of methylene blue and phenol, *Chemical Engineering Journal*, **124**, 103-110.

Fitzer E., Schäfer W., (1970), The effect of crosslinking on the formation of glasslike carbons from thermosetting resins, *Carbon*, **8**, 353-364.

Frąckowiak E., Metenier K., Bertagna V., Beguin F., (2000), Supercapacitor electrodes from multiwalled carbon nanotube, *Applied Physics Letters*, **77**, 2421-2423.

Fuertes A.B., (2004), Synthesis of ordered nanoporous carbons of tunable mesopore size by templating SBA-15 silica materials, *Microporous and Mesoporous Materials*, **67**, 273-281.

Gadiou R., Saadallah S., Piquero T., David P., Parmentier J., Vix-Guterl C., (2005), The influence of textural properties on the adsorption of hydrogen on ordered nanostructured carbons, *Microporous Mesoporous Materials*, **79**, 121-128.

Gierszal K.P., Jaroniec M., Kim T.W., Kim J., Ryoo R., (2008), Carbon nanofibers, *New Journal of Chemistry*, **32**, 981-993.

Gomez S.V., Piriz A.F., Duran V.C., Pastor V.J., (1999), Formation of oxygen structures by air activation. A study by FT-IR spectroscopy, *Carbon*, **37**, 1517-1528.

Guo L., Zhang L., Zhang J., Zhou J., He Q., Zeng S., Cui X., Shi J., (2009), Hollow mesoporous carbon spheres - an excellent bilirubin adsorbent, *Chemical Communications*, **40**, 6071-6073.

Hwang S.W., Hyun S.H., (2004), Capacitance control of carbon aerogels, *Journal of Non-Crystalline Solids*, **347**, 238-245.

Hartmann M., Vinu A., (2002), Mechanical stability and porosity analysis of large-pore SBA-15 mesoporous molecular sieves by mercury porosimetry and organics adsorption, *Langmuir*, **18**, 8010-8016.

Idris J., Osman S.F., Christian C., (2017), A comparison of water filtering materials made from extracted palm fruit fibre and palm kernel shell, *Environmental Engineering and Management Journal*, **16**, 2657-2663.

Ignat M., Van Oers C.J., Vernimmen J., Mertens M., Potgieter V.S., Meynen V., Popovici E., Cool P., (2010), Textural property tuning of ordered mesoporous carbon obtained by glycerol conversion using SBA-15 silica as template, *Carbon*, **48**, 1609-1618.

Joo S.H., Choi S.J., Oh I., Kwak J., Liu Z., Terasaki Q., Ryoo R., (2001), Ordered nanoporous arrays of carbon supporting high dispersions of platinum nanoparticles, *Nature*, **412**,169-172.

Karabacakoglu B., Tumsek F., Demiral H., Demiral I., (2008), Liquid phase adsorption of phenol by activated carbon derived from hazelnut bagasse, *Journal of International Environmental Application &Science*, **3**, 373-380.

Kim H., Kim P., Joo J.B., Kim W., Song I. K., Yi J., (2006), Fabrication of a mesoporous Pt-carbon catalyst by the direct templating of mesoporous Pt-alumina for the methanol electro-oxidation, *Journal of Power Sources*, **157**, 196-200.

Kim T., Park I., Ryo R., (2003), A synthetic route to ordered mesoporous carbon with Graphitic Pore Walls, *Angewandte Chemie*, **115**, 4511-4515.

Kim T.W., Ryoo R., Gierszal K.P., Jaroniec M., Solovyov L.A., Sakamoto Y., Terasaki O., (2005), Characterization of mesoporous carbons synthesized with SBA-16 silica template, *Journal of Materials Chemistry*, **15**, 1560-1571.

Kim D.J., Lee H.I., Yie J.E., Kim S.J., Kim J.M., (2005), Ordered mesoporous carbons: Implication of surface chemistry, pore structure and adsorption of methyl mercaptan, *Carbon*, **43**, 1868-1873.

Li H., Xi H., Zhu S., Wen Z., Wang R., (2006), Preparation, structural characterization, and electrochemical properties of chemically modified mesoporous carbon, *Microporous and Mesoporous Materials*, **96**, 357-362.

Martin A., Manfred R., (2011), Oligomerization of glycerol – a critical review, *European Journal of Lipid Science and Technology*, **113**, 100-117.

Palanichamy R., Senthil K.P., Muthukumar P., Dinesh K.S., Palanichamy B., Subramanian S., (2014), Removal of Cu(II) ions from aqueous solution by adsorption onto activated carbon produced from Guazuma Ulmifolia Seeds, *Environmental Engineering and Management Journal*, **13**, 905-914.

Ryoo R., Joo S.H., Jun S., (1999), Synthesis of highly ordered carbon molecular sieves via template-mediated structural transformation, *Journal of Physical Chemistry B*, **103**, 7743-7746.

Ryoo R., Joo S.H., Kruk M., Jaroniec M., (2001), Ordered Mesoporous Carbons, *Advanced Materials*, **13**, 677-681.

Secula M.S, Dávid E., Cagnon B., Vajda A., Stan C., Mămăligă I., (2018), Kinetics and equilibrium studies of 4-chlorophenol adsorption onto magnetic activated carbon composites, *Environmental Engineering and Management Journal*, **17**, 783-793.

Shawabkeh R.A., Abu-Nameh E.S.M., (2007), Absorption of phenol and methylene blue by activated carbon from pecan shells, *Colloid Journal*, **69**, 355-359.

Soltani S.M., Yazdi S.K., Hosseini S., (2013), Effects of pyrolysis conditions on the porous structure construction of mesoporous charred carbon from used cigarette filters, *Applied Nanoscience*, **4**, 551-569.

Suzuki M., (1994), Activated carbon fiber: Fundamentals and applications, *Carbon*, **32**, 577-586.

Vaudreuil S., Bousmina M., Kaliaguine S., Bonneviot L., (2001), Synthesis of macrostructured MCM-48 molecular sieves, *Microporous and Mesoporous Materials*, **44-45**, 249-258.

Wang T., Liu X., Zhao D., Jiang Z., (2004), Recent advances in biocompatible supramolecular assemblies for biomolecular detection and delivery, *Chemical Physics Letters*, **389**, 327-331.

Wu D., Liang Y., Yang X., Li Z., Zou C., Zeng X., Lv G., Fu R., (2008), Direct fabrication of bimodal mesoporous carbon by nanocasting, *Microporous and Mesoporous Materials*, **116**, 91-94.

Xiao B., Thomas K.M., (2005), Adsorption of aqueous metal ions on oxygen and nitrogen functionalized nanoporous activated carbons, *Langmuir*, **21**, 3892-902.

Zhang W., Lu J., Han B., Li M., Xiu J., Ying P., Li C., (2002), Direct synthesis and characterization of titanium-substituted mesoporous molecular sieve SBA-15, *Chemistry of Materials*, **14**, 3413-3421.